

COMMISSIONING OF THE FERMI@ELETTRA LASER HEATER*

Simone Spampanati[#], Sincrotrone Trieste, Italy,
 University of Nova Gorica, Nova Gorica, Slovenia, SLAC, Menlo Park, CA 94025, U.S.A
 Enrico Allaria, Laura Badano, Silvano Bassanese, Davide Castronovo, Miltcho B. Danailov,
 Alexander Demidovich, Simone Di Mitri, Bruno Diviacco, William M. Fawley, Lars Froelish,
 Giuseppe Penco, Carlo Spezzani, Mauro Trovò, Sincrotrone Trieste, Italy
 Giovanni DeNinno, Eugenio Ferrari,
 Sincrotrone Trieste, Italy, University of Nova Gorica, Nova Gorica, Slovenia
 Luca Giannessi, ENEA C.R. Frascati, Frascati (Roma) Italy, Sincrotrone Trieste, Italy.

Abstract

The linac of the FERMI seeded free electron laser includes a laser heater to control the longitudinal microbunching instability, which otherwise is expected to degrade the quality of high brightness electron beam sufficiently to reduce the FEL power. The laser heater consists of a short undulator located in a small magnetic chicane through which an external laser pulse enters to modulate the electron beam energy both temporally and spatially. This modulation, which varies on the scale of the laser wavelength, together with the effective R52 transport term of the chicane increases the incoherent energy spread (i.e., e-beam heating). We present the first commissioning results of this system, and its impact both upon the electron beam phase space, and upon the FEL output intensity and quality.

INTRODUCTION

FERMI@ELETTRA [1] is a user facility based on two seeded FELs in the VUV (FEL-1) and soft x-ray (FEL-2) wavelength regimes. FEL-1 is a single stage HGHG while FEL-2 is a two stage HGHG cascade working in a fresh bunch configuration. One of the main features of both the two FEL lines is their capability to produce output radiation pulses with a very narrow spectrum. The longitudinal high quality of the output FEL pulses originates with the external seed laser. However, the nearly transform-limited single spike spectrum [2] can be spoiled by unwanted modulations and distortions in the longitudinal phase space of the electron beam. The very bright electron beam (e.g., slice emittance <math><2\text{ mm mrad}</math>) and incoherent energy spread ($\sim 3\text{ KeV}$) required to drive this FEL is susceptible to a microbunching instability [3] that produces short wavelength ($\sim 1\text{-}5\mu\text{m}$) energy and current modulations. These can both degrade the FEL spectrum and reduce the power by increasing the slice energy spread. This instability is presumed to start at the photoinjector exit growing from a pure density modulation caused by shot noise and/or unwanted modulations in the photoinjector laser temporal profile.

* Work supported in part by the Italian Ministry of University and Research under grants FIRB-RBAP045JF2 and FIRB-RBAP06AWK3
[#] spampana@slac.stanford.edu

As the electron beam travels along the linac to reach the first bunch compressor (BC1), the density modulation leads to an energy modulation via longitudinal space charge. The resultant energy modulations are then transformed into higher density modulations by the bunch compressor. The increased current non-uniformity leads to further energy modulations along the rest of the linac. Coherent synchrotron radiation in the bunch compressor can further enhance these energy and density modulations. To control these degradations, we have installed a laser heater between the photoinjector and the linac. This device can add a small controlled amount of incoherent energy spread to the beam and reduces microbunching instability growth via Landau Damping in the bunch compressor.

LASER HEATER SET UP

The FERMI laser heater [4] consists of a short, planar-polarized undulator located in a magnetic chicane through which an external laser pulse enters to modulate the electron beam both temporally and spatially. The resulting interaction within the undulator produces an energy modulation of the electron beam on the scale of the laser wavelength. The last half of the chicane then time-smears the energy modulation leaving an effective incoherent energy spread increase. Figure 1 shows the FERMI layout with the laser heater positioned between the photoinjector and the linac. Figure 2 illustrates the laser heater system installed in the linac tunnel.

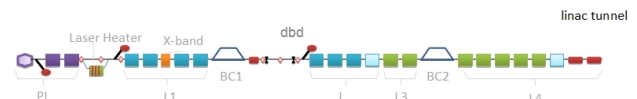


Figure 1: FERMI linac layout.

The laser heater undulator has 12 periods of 4cm. The gap can be changed to find the resonance with the external laser wavelength (783nm) for several beam energy. The relative bandwidth of undulator radiation is $\sim 8\%$ while the gap-K calibration has an error of the order of 0.3%. A nearby spectrometer allows determination of the electron beam energy to within 1%. Consequently it is

very easy to find the resonance with an acceptable accuracy.

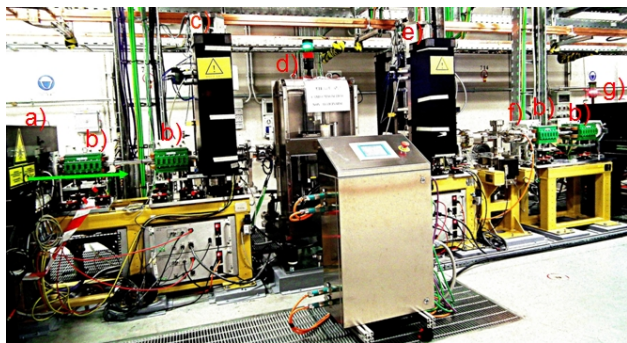


Figure 2: Laser heater system in the lynac tunnel : a) input laser table, b) chicane magnet; c) multiscreen station LH01.02, d) laser heater undulator; e) multiscreen station LH01.03, f) bpm LH01.03, g) output laser table.

The laser pulse used for the laser heater is a small portion of the photocathode infrared drive laser picked up just before the harmonic up-conversion to UV. Up to $160\mu\text{J}$ of energy are available for the laser heater after the beam transport; with a FWHM duration of 10 ps, this corresponds to a peak power of 16 MW. According to theory, this level of power level will produce 100-keV of energy spread.

Table 1: Laser Heater Parameter

Parameter	Value	Units
Undulator period	40	mm
Number of periods	12	-
Undulator strength parameter	1.17-0.8	-
Laser wavelength	783	nm
Laser pulse duration	10	ps
Laser energy	<160	μJ
Laser rms transverse size	140-200	μm
X Offset in the chicane	30	mm
Chicane bending angle	3.5	Degrees

The nominal value of beam heating required by FEL operations according to simulations is around 10 keV but we started the commissioning of the laser heater at full power to detect more clearly the heating. The laser is transported on an optical table placed in the linac tunnel near the electron beam vacuum pipe and before the heater chicane. Two mirrors located on this table steer the laser beam to overlap the electron beam trajectory. Another optical table is placed on the other side of the heater chicane to host additional diagnostics. Two multiscreen diagnostic stations, one on each side of the undulator, lay within the laser heater chicane. Both diagnostic stations are equipped with CROMOX screens on which it is

possible to image both the laser beam and the electron beam in order to superimpose them transversely. Three remote controllable mirrors, one in the laser room and two on the optical table at the laser heater chicane entrance, permit adjustment of the laser centroid position relative to that of the electron centroid to within $100\mu\text{m}$ tolerance. Since both the electron beam and laser heater laser originate with the photocathode laser, they are naturally locked in time but with a constant temporal offset that can be adjust scanning a delay to superimpose the two beams temporally.

MEASUREMENTS OF THE BEAM HEATING

When the electron beam and the laser beam are aligned in space and time, the laser electron interaction in the undulator generates significant energy spread that is easily detected using the spectrometer placed after the first bunch compressor. The beam is deflected vertically with a vertical RF [5] before entering the spectrometer. This deflection maps the longitudinal coordinate to the vertical coordinate on the spectrometer YAG screen while the dipole spectrometer converts the energy of the beam to the horizontal coordinate on the same screen. The spectrometer has a dispersion $\eta \approx 0.58\text{ m}$ and a small beta function ($\beta \approx 1\text{ m}$) on the diagnostic YAG screen. On the screen it is possible to see the longitudinal phase space of the beam enabling measurement of the uncorrelated energy spread in each slice along the longitudinal coordinate (time) of the electron beam. Figure 4 shows representative longitudinal phase space profiles on the on the spectrometer screen when the laser heater is switched off and when the beam is heated by the laser at full energy ($160\mu\text{J}$). The transverse rms dimension of the laser in the undulator is around $\sim 200\mu\text{m}$ while electron beam sigma is $\sim 140\mu\text{m}$. The heated beam is expected to show a double horn energy distribution when the laser electric field is larger than the electron beam as shown in figure 3. The energy distribution is more Gaussian-like when the laser matches electron beam size in the undulator; this configuration has been shown to be more effective in suppressing the microbunching instability [6]. However, we started with a large laser spot to more easily overlap the electron beam. Figure 4 shows the evolution of the energy spread of a central slice of the beam as a function of the laser behaviour [7]. The values showed by the blue experimental points are obtained by subtracting in quadrature the energy spread measured with heater off from the value measured with heater on; in principal the difference is equivalent to the energy spread added by the laser heater. The magenta line shows the expected theoretical behaviour. The experimental points (blue) are obtained subtracting in quadrature the energy spread measured with the heater switched off from the energy spread measured with the heater on. One sees that there is excellent agreement with the theoretically predicted values.

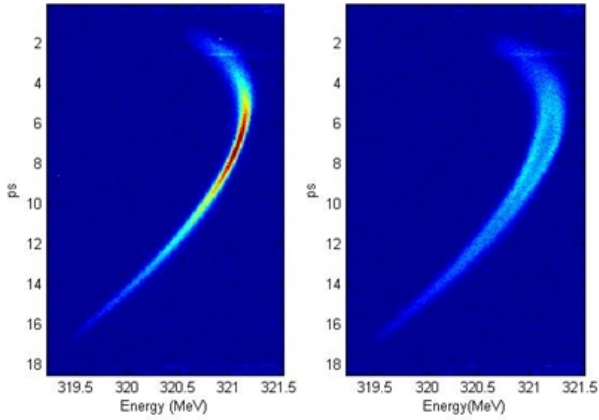


Figure 3: Longitudinal electron beam phase space reconstructed on the spectrometer screen with the RF deflector on. Left image: laser heater off. Right image: heater on with a laser energy of 160μJ.

The error bars are obtained from the statistical measurement errors on 15 shots and from estimated errors on energy and dispersion measurements (1% and 5%). We note excellent agreement between theory and measured data. The measurements reported were taken with the gap optimized experimentally for maximum beam heating.

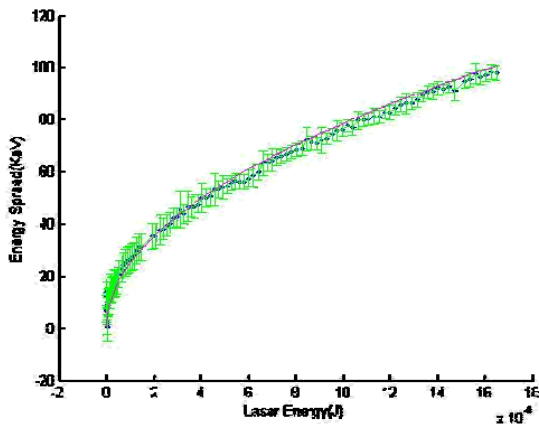


Figure 4: Behaviour of the electron beam energy spread added by the heater vs. the laser energy. The magenta line shows the expected theoretical behaviour. The experimental points (blue) are obtained subtracting in quadrature the energy spread measured with the heater switched off from the energy spread measured with the heater on.

MICROBUNCHING SUPPRESSION

Now we analyze the effect of the laser heater on the electron beam evolution downstream. All the results presented here are obtained while operating the linac with only BC1 on. Clear evidence of microbunching instability effects can be seen when the linac is set to a compression factor greater than 3 as both the current and energy

spectrum of the beam appear to be modulated. Figure 5 shows the electron beam energy profiles imaged on the screen of the spectrometer in the diagnostic beam dump (DBD) at the end of the linac for various settings of the laser heater energy. These data were acquired for a 500-pC beam charge with a compression factor of 5.6. The x-band linearization cavity was switched off resulting in the compression non-linearities producing a triangular current distribution and other long scale non-uniformities. The DBD spectrometer screen images show a residual energy chirp with the energy profile sensitive to the beam current profile. The magenta curve in the Fig. 5a displays the energy profile measured with the heater switched off. It shows high frequency modulations we attribute to the microbunching instability and also longer time scale structures produced by non-linearities in beam compression. When the laser heater is turned on with a laser energy $\sim 1\mu\text{J}$, the high frequency structures start to be reduced in amplitude (Fig. 5b) whereas the longer current structure are almost untouched by this small level of heating. When the laser energy is increased to a level of $\sim 3\mu\text{J}$ or greater, even longer scale structures are smeared and reduced as reproduced in Fig. 5c.

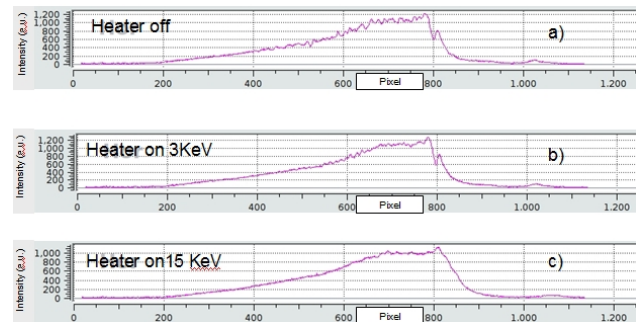


Figure 5: Energy beam profiles imaged on the screen of the spectrometer in the diagnostic beam dump (DBD in the Fig. 1) for various setting of the laser heater.

Other evidence for microbunching instability growth is the coherent optical transition radiation (COTR) produced when the beam passes through diagnostic OTR screens [8]. The laser heater reduces and eventually suppresses these COTR signals. Figure 6 reproduces the behaviour of the OTR signal just upstream of the FEL-1 modulator undulator as a function of laser heater energy; one sees strong suppression of the signal for energies exceeding 1 μJ.

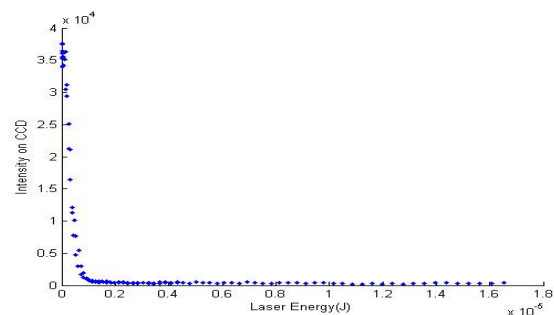


Figure 6: OTR intensity vs. laser heater energy.

EFFECTS ON FEL PERFORMANCE

Beneficial effects of the laser heater have been observed on both the FEL pulse energy and spectrum. The FEL pulse energy at 24.3 nm (10th harmonic of the seed produced by an optical parametric amplifier tuned at 243nm) measured on a downstream gas cell vs. the seed laser energy is shown in Fig. 7 for three different settings of the laser heater.

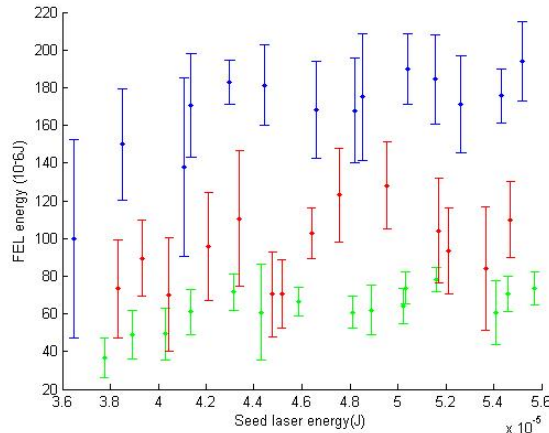


Figure 7: FEL pulse energy at 24.3 nm vs. seed energy. The green points were taken when the laser heater is switched off. The red points refer to a beam heating of 14 keV while the blue points correspond to a beam heating of 7 keV.

These data were obtained with a 500 pC electron beam charge at a compression factor close to 10 in BC1. Here the X-band cavity was turned on and tuned to produce a nominally linearized compression. The maximum FEL output energy is more than doubled at the optimum laser heater setting (7-keV equivalent heating) as compared to that obtained when the laser heater is switched off. These results confirm that the laser heater increases the electron beam quality and suggests that the slice energy spread at undulator entrance is minimized by a proper amount of upstream heating as predicted by theory and simulation [9]. The laser heater produces even a “cleaning” of the FEL spectrum. Fig (8) shows 100 spectra taken with the laser heater switched on (top plot) and 100 spectra taken with the laser heater turned off (bottom plot). The black lines in the two plots are the mean of the ensemble. For these data the electron beam charge is 500 pc and the BC1 compression factor ~ 10 . The radiator is tuned on the 8th harmonic of the seed laser. On a shot-by-shot basis, when the laser heater is off the FEL spectrum has a spiky aspect with multiple peaks associated with strong energy modulation of the electron beam phase space. By contrast, when the laser heater is switched on the spectra appear cleaner with Gaussian-like shapes and the central wavelength is also more stable.

We also found a positive effect upon the FEL power even when working with lower compression factors and for longer wavelengths. As example we report an energy

gain of 50% switching on the laser heater for a compression factor ~ 3 and at a wavelength of 52 nm. As with the higher compression cases discussed above, the optimal laser heating for maximizing FEL power is in the range of 7 to 14 keV. Operations at very high harmonic of the seed (26-29th) require lower laser heater energy (3-5 keV).

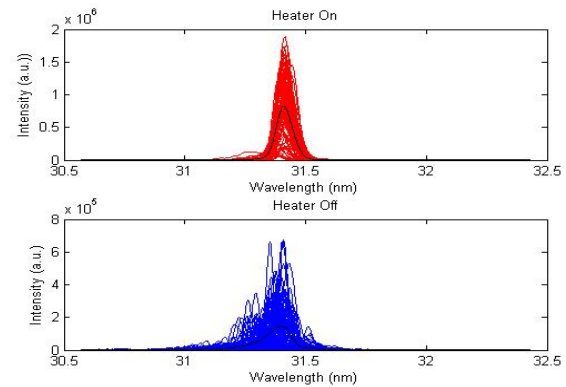


Figure 8: FEL output spectra at the 8th harmonic of the external seed laser. Top panel: heating on; bottom panel: heating off.

ACKNOWLEDGMENTS

We thank P. Craievitch, A. Lutman and M. Petronio for their work to project and commission the RF deflector used in this work. We also thank M. Venturini and A. Zholents for their studies of the microbunching instability in the FERMI@ELETTRA linac.

CONCLUSIONS

The laser heater system for the FERMI@ELETTRA has been commissioned. The system works more or less as predicted with beneficial effects upon both the FEL output power and spectrum. The heating also appears to reduce microbunching instability growth as seen both in suppression of COTR emission and also in terms of short time scale structure on the electrons beam’s energy distribution. The optimal heating in terms of the induced energy spread growth is at the 7-14 keV level.

REFERENCES

- [1] E. Allaria, C. Callegari, D. Cocco, W. M. Fawley, M. Kiskinova, C. Masciovecchio and F. Parmigiani, *New J. Phys.* 12, 075002 (2010).
- [2] E. Allaria et al., TUOB04, These proceedings.
- [3] E.L.Saldin, E.A.Schneidmille, M-V.Yurkov, *NIMA* 409,1,(2002).
- [4] S.Spampinati, S.Di Mitri, B. Diviacco, FEL conference 2007.
- [5] P. Craievivh et al., FEL conference 2010.
- [6] Z.Huang et al., *Phys. Rv. STAB*, 7, 074401 (2004).
- [7] Z.Huang et al., *Phys. Rv. STAB*, 12, 020703 (2010).
- [8] R.B. Fiorito, FEL conference 2009.
- [9] S. Dimitri et al., *Nucl.Instrum.Meth.A608:19-27,2009.*